AN APPLICATION TO AUTOMATE REFERENCE FRAME TRANSFORMATIONS IN HIGH-ENERGY AND NUCLEAR PHYSICS

by

George Vassilakopoulos

A Thesis Submitted to the Faculty of the Department of Physics
Old Dominion University in Partial Fulfillment of the
Requirements for the Degree of

BACHELOR OF SCIENCE

PHYSICS

OLD DOMINION UNIVERSITY
May 2026

Approved by:

Ted Rogers Digitally signed by Ted Rogers Date: 2025.05.09 08:04:05 -04'00'

Ted Rogers (Director)

Arkaitz Rodas Bilbao Digitally signed by Arkaitz Rodas Bilbao Date: 2025.05.08 20:39:12 -04'00'

Arkaitz Rodas (Member)

Balsa Terzic

Balsa Terzic (Member)

ABSTRACT

AN APPLICATION TO AUTOMATE REFERENCE FRAME TRANSFORMATIONS IN HIGH-ENERGY AND NUCLEAR PHYSICS

George Vassilakopoulos
Old Dominion University, 2025
Director: Dr. Ted Rogers

In high-energy and nuclear physics, analyzing the behavior and substructure of final state particles, such as hadronic jets, is critical to understanding the dynamics of quarks and gluons (so-called "partons") governed by Quantum Chromodynamics (QCD) in highly relativistic collisions. These final states, observed in particle collider experiments, emerge from the fragmentation and hadronization of energetic partons and are studied theoretically in specific reference frames. This thesis presents a MATLAB-based application developed to automate and visualize Lorentz and rotational transformations. The application enables users to define input four-vectors and perform precise relativistic boosts and rotations to focus on specific final state structures in relativistic particle collisions. It leverages compact analytic expressions for transformation matrices, offering flexibility for a wide range of physical scenarios. Demonstrations involving electron-positron annihilation and proton-proton collision-inspired examples illustrate the application's capability to transform lab frame vectors to new frames optimized for QCD analyses. This tool enhances the interpretability of final state observables by streamlining these transformations and providing interactive 3D and 2D visualizations of vectors before and after frame shifts. It is particularly useful for theoretical investigations and experimental comparisons involving jet substructure, fragmentation functions, and parton distribution functions.

ACKNOWLEDGMENTS

This work was supported by the U.S. Department of Energy, Office of Science, Office of Nuclear Physics, under Award Number DE-SC0024715. I want to thank my committee members, Dr. Terzic and Dr. Rodas, for their feedback on this manuscript. The guidance and efforts of my directing advisor, Dr. Rogers, deserve special recognition. This project would not be possible without him.

TABLE OF CONTENTS

Page

LIST OF FIGURES

CHAPTER 1

INTRODUCTION

1.1 BACKGROUND

Quantum Chromodynamics (QCD) is the fundamental theory in particle physics that describes the strong interaction, one of the four fundamental forces of nature. The strong interaction governs how quarks and gluons (so-called "partons") interact. QCD exhibits three main properties that govern its behavior: confinement, asymptotic freedom, and chiral symmetry breaking.

Confinement imposes that color-charged particles, such as quarks and gluons, cannot exist in isolation. The force-carrying gluons of QCD carry a color charge unlike Quantum Electrodynamic (QED) charged particles. QED particles experience an electric field whose strength decreases as particles separate in distance. On the other hand, the gluon field between a pair of color charges forms a narrow flux tube (or string) between them. Because of this behavior of the gluon field, the strong force between the particles is constant regardless of their separation. Therefore, as quarks separate to try and exist in isolation, it becomes more favorable for their tube to "snap" and form a quark-antiquark pair.

Asymptotic freedom and chiral symmetry breaking describe the behavior of QCD across energy scales. Asymptotic freedom is the property that the strong interaction weakens at high energies or short distances, allowing quarks and gluons to behave almost as free particles, a property crucial for high-energy particle collisions. Conversely, the strong force becomes stronger at low energies or large distances, confining quarks and gluons within hadrons. At this scale, QCD's approximate chiral symmetry is spontaneously broken by the non-trivial structure of the QCD vacuum, resulting in the formation of a quark condensate and giving rise to pseudo-Goldstone bosons, such as pions, kaons, and etas [2]. These phenomena together capture the dual nature of QCD: perturbative at high energies and non-perturbative at low energies, shaping the fundamental interactions and structure of matter.

Hadronic jets are essential observables in high-energy collisions, serving as direct signatures of quarks and gluons produced in hard scatterings. These collimated sprays of hadrons arise from the fragmentation and hadronization of energetic partons, processes governed by Quantum Chromodynamics (QCD). Despite the complexity of hadronization, the overall energy and momentum distributions of jets remain closely linked to their initiating partons, allowing for detailed studies of QCD dynamics [3]. Early observations of jet structures in electron-positron collisions at PETRA and SLAC, followed by precision measurements at the Large Electron-Positron Collider (LEP) and hadron colliders like the LHC, have established jets as a fundamental tool for probing the strong interaction [4].

The internal composition and number of jets in a collision depend on the energy and type of particles involved. In a simple scenario, a quark-antiquark pair produces two jets, but more complex interactions can lead to additional jets through gluon radiation [4]. Proton-proton collisions, such as those at the LHC, involve partons carrying unknown momentum fractions, leading to varying jet multiplicities and energies. In contrast, electron-positron collisions, like those at LEP, provide a cleaner environment with simple leptonic initial states, producing predominantly two jets unless additional radiation occurs. The absence of Parton Distribution Functions (PDFs) in electron-positron collisions makes them ideal for precision studies of fragmentation functions, which can then be applied to more complex systems, such as electron-proton or hadron-hadron collisions. By applying these transformations, researchers can better study individual jet dynamics, distinguishing them from the global event properties and enhancing our understanding of the fundamental forces that govern particle interactions.

1.2 MOTIVATION

Hadronic jets are essential observables in high-energy collisions, serving as the experimental signatures of quarks and gluons produced in hard scatterings. These collimated sprays of hadrons result from the fragmentation and hadronization of energetic quarks and gluons, processes governed by the strong interaction described by Quantum Chromodynamics (QCD). Figure 1 illustrates the concept of factorization [1] in high-energy electron-positron collisions, where complex hadronic final states can be approximated and analyzed in terms of their originating quarks and gluons. Since quarks and gluons can never be observed and studied directly, anything

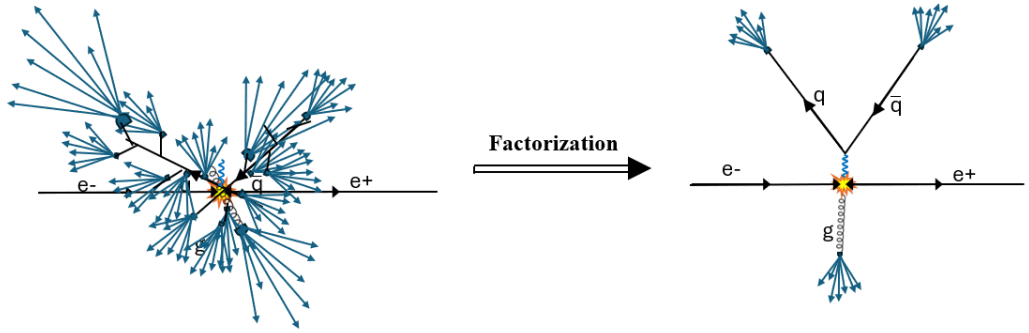

FIG. 1: Diagram of an electron-positron collision. The left-hand side is a cartoon depiction of what the true structure of such a process might be. The right-hand side is the way it is viewed within the theoretical procedure known as "factorization" [1], where hadrons are approximately lumped into discrete clusters associated with definite quarks and gluons. An issue that needs to be addressed by theorists is the question of how the approximations used in factorization affect the kinematics of the process.

we learn about them must come indirectly from the study of complicated final-state hadronic observables like these. On the left of the figure, the intricate structure of hadronic jets emerges from the fragmentation and hadronization of the quark, antiquark, and radiated gluon. However, by applying the theoretical technique of "factorization," [1] as depicted on the right, the complicated hadron-level picture is reduced to a more manageable partonic representation, where individual jets are linked to specific initiating partons. This simplification allows for the application of theoretical objects like fragmentation functions (see a discussion of these below), which describe the probability of a parton transforming into observed hadrons, helping researchers extract fundamental QCD parameters. Additionally, to utilize these techniques, relativistic reference frame transformations must be used to isolate individual jets from the rest of the event dynamics, allowing for a clearer interpretation of jet substructure and momentum flow, and other final state properties. Combined with other approximations, such as the collinear factorization framework and perturbative QCD calculations, this procedure refines our ability to study the underlying partonic interactions while minimizing contamination from soft and non-perturbative effects.

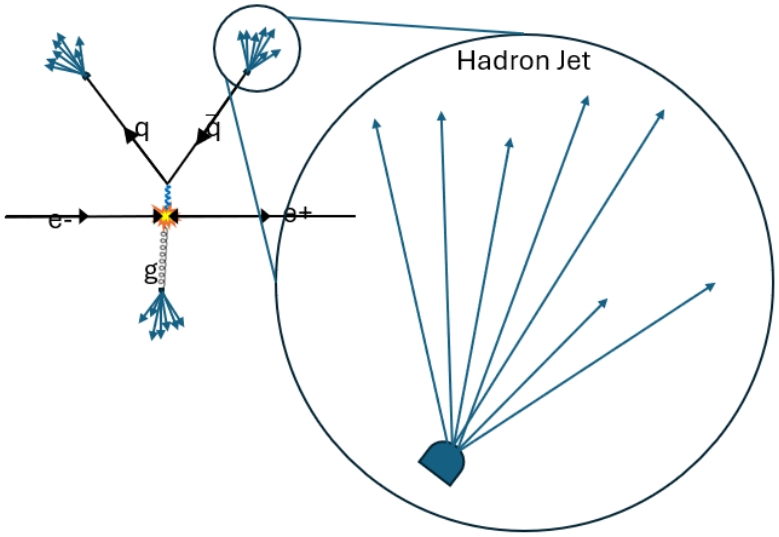

FIG. 2: Factorization theorems focus on individual clusters of hadrons and characterize the properties of "jets" or fragmentation functions. For example, a theorist who wishes to understand the properties of a single quark and how it transforms into a cluster of hadrons will focus only on the part in the circle, with the hope that it has minimal sensitivity to other parts of the final state.

Despite the complexity of hadronization, the overall energy and momentum distributions of jets are closely linked to their initiating partons, allowing jets to be studied in terms of their underlying QCD dynamics. Early discoveries of jet structures in electron-positron collisions at PETRA and SLAC, followed by precision measurements at the Large Electron-Positron Collider (LEP) and hadron colliders like the LHC, have confirmed that jets provide a robust framework for probing the fundamental nature of strong interactions.

To analyze the properties of individual jets in a collision event, it is often necessary to apply reference frame transformations that isolate a jet's motion from the broader event dynamics, seen in Figure 2. Since collider experiments operate in different kinematic regimes, such as electron-positron annihilation, where the center-of-mass frame is well-defined, versus hadron collisions, where incoming partons carry unknown momentum fractions, choosing an appropriate reference frame is crucial. Transformations such as Lorentz boosts and rotations allow for a clearer interpretation of jet momentum, substructure, and energy flow, independent of the global event

characteristics. By studying final states like these in optimal reference frames, one can extract more precise information about their formation, improve comparisons with theoretical predictions, and enhance searches for new physics phenomena that may manifest within jet structures.

One particularly useful reference frame transformation in jet studies is the boost to the jet rest frame, where the total momentum of a selected jet is set to zero. This transformation allows researchers to examine the internal substructure of the jet without needing to refer to the detailed kinematics of the overall scattering process. For example, consider a high-energy proton-proton collision at the LHC that produces a quark-antiquark pair. Each quark hadronizes into a separate jet, but due to the complex momentum distribution of the initial protons, these jets are often produced with significant boosts along the beam axis. By applying a Lorentz boost to the rest frame of one of these jets, researchers can study its fragmentation pattern, energy flow, and substructure independent of the overall motion imparted by the collision.

The fragmentation function formalism is a complementary approach to the jet concept. A fragmentation function is a probability density to find a particular type of hadron in the final state remnants of a quark or gluon. It depends on the fraction of the largest component of quark momentum carried by the hadron and is usually expressed as

$$D_{h/i}(\xi) \tag{1}$$

where h is the type of hadron, i is the type of quark or gluon, and ξ is the momentum fraction

$$\xi = \frac{p_h^+}{k^+}, \tag{2}$$

where p_h^+ is the "plus" momentum (see next section) of the hadron h and k^+ is the plus momentum of the quark or gluon in a frame where it is moving fast along the +z axis [5].

One of the most commonly studied fragmentation functions is the pion fragmentation function, which describes how quarks or gluons fragment into pions (π^+, π^-, or π^0). A widely used fragmentation function in QCD is the leading-order parameterization for the fragmentation of a quark into a pion:

$$D_{h/i}(\xi, Q^2) = N\xi^\alpha(1-\xi)^\beta \tag{3}$$

where Q^2 is the energy scale of the process and N, α, and β are phenomenological

parameters determined from experimental data. In the case, if $\xi \ll 1$, the hadron carries only a small fraction of the original quark's momentum, meaning many low-energy hadrons are produced. If $\xi \approx 1$, the hadron takes nearly all of the quark's momentum, but such events are less probable due to the suppression by the third factor in Equation 3. The fragmentation function evolves with the energy scale Q^2, meaning that at higher energies, more hadrons are produced, and their energy is distributed over a broader range.

The choice of reference transformation depends on the research focus. Suppose a researcher is interested in the momentum distributions of individual jet constituents. In that case, they may perform a transformation to the jet rest frame, allowing them to study how the jet's energy is shared among its particles. In contrast, if the goal is to compare jets across different collision systems (e.g., e^+e^- vs. pp collisions), a transformation to a frame where the jet's transverse momentum is fixed can help normalize kinematic effects and facilitate direct comparisons. Similarly, in searches for boosted heavy particles, such as a Higgs boson decaying into a pair of bottom quarks, it is useful to transform to a frame where the parent particle is at rest, helping to reconstruct its invariant mass with minimal contamination from the motion of its decay products.

Ultimately, different researchers prioritize different aspects of jet behavior based on their scientific objectives—precision QCD studies, new physics searches, or comparisons between theoretical predictions and experimental data. The choice of reference frame transformation is thus a key methodological decision that enables the most relevant and insightful analysis of jet dynamics.

1.3 REVIEW OF THE BASIC FORMALISM

In the context of the desired transformation for my application, it is convenient to use the light-cone coordinates, which I will define here. They are a reformulation of the usual Minkowski space (t, x, y, z), particularly useful when a system has a preferred axis and is highly relativistic, typically the z-axis, which is the beam direction in a collider experiment. Instead of using conventional time and space coordinates, one defines light-cone coordinates as follows:

$$V^+ = \frac{1}{\sqrt{2}}(V^0 + V^z), \tag{4}$$

$$V^- = \frac{1}{\sqrt{2}}(V^0 - V^z), \tag{5}$$

$$\mathbf{V}_\mathrm{T} = (V^x, V^y)\,. \tag{6}$$

Here, V^+ and V^- are called the light-cone components, while $\boldsymbol{V}_\mathrm{T}$ represents the transverse momentum components. The introduction of these variables makes certain relativistic calculations more straightforward, especially in scenarios involving highly boosted particles. Figure 3 displays the two light-cone coordinate axes relative to a space-time diagram. The two axes lie along the world line of light in the positive and negative z-direction.

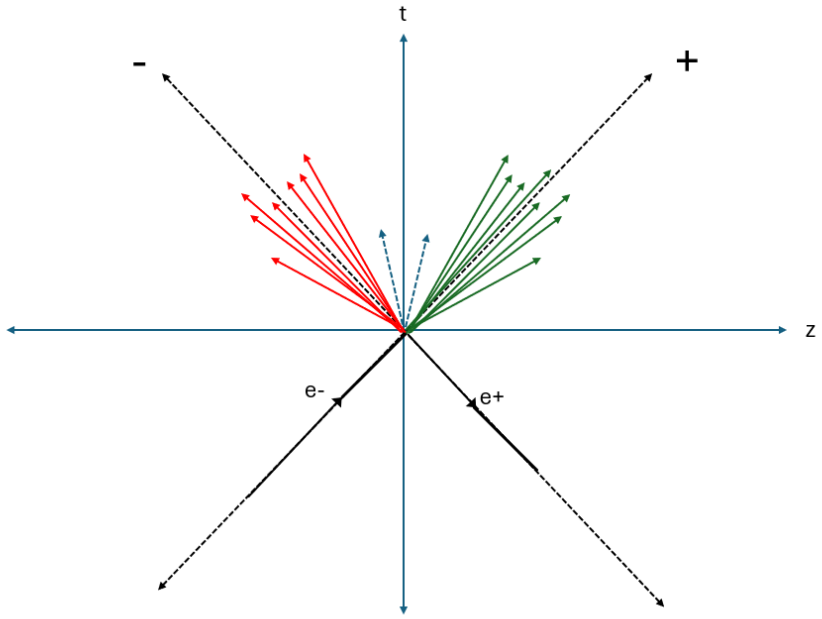

FIG. 3: Space-time diagram with light-cone coordinate axes is shown schematically for visualization. An e^+e^- collision occurs at $t = 0$ and produces a pair of jets with back-to-back rapidity. The two dotted vectors represent possible unknown quarks that could emerge from the collisions that are unaccounted for.

Scalar products play a fundamental role in relativistic physics, as they allow for the calculation of invariant quantities. The scalar product of two four-vectors V and

W in Minkowski space is usually written as

$$\begin{aligned} V \cdot W &= g_{\mu v} V^{\mu} W^{v} \\ &= V^0 W^0 - V^x W^x - V^y W^y - V^z W^z \end{aligned} \tag{7}$$

The products generally involve the original coordinates multiplied by a transformation matrix. In the case of equation (4), the vectors are multiplied by the Minkowski space-time metric, $g_{\mu\nu}$. In light-cone coordinates, the product becomes

$$V \cdot W = V^+ W^- + V^- W^+ - \boldsymbol{V}_{\mathrm{T}} \cdot \boldsymbol{W}_{\mathrm{T}} \,. \tag{8}$$

This form is particularly useful in high-energy physics because it separates the longitudinal and transverse contributions. When a particle is highly boosted in the z-direction, only one of the light-cone coordinates will dominate, making it easier to analyze energy and momentum transfers in scattering processes.

The convenience of light-cone coordinates produces simple Lorentz boosts: a simple multiplication of the original plus and minus coordinates with a rapidity exponential, e^y and e^{-y}, respectively. Let us boost the coordinates in the z direction to a new primed system, V'^{μ}. In the ordinary four-vector components, there are the well-known formulae

$$V'^0 = \frac{V^0 + v V^z}{\sqrt{1 - v^2}} \,, \tag{9}$$

$$V'^z = \frac{v V^0 + V^z}{\sqrt{1 - v^2}} \,, \tag{10}$$

$$V'^x = V^x \,, \tag{11}$$

$$V'^y = V^y \,. \tag{12}$$

The boost in light-coordinates derives to the following:

$$V'^+ = V^+ e^{\psi}, \tag{13}$$

$$V'^- = V^- e^{-\psi}, \tag{14}$$

$$V'_T = V_T. \tag{15}$$

The boost to the new light-cone coordinates depends only on the original component and the hyperbolic angle, $\psi = \frac{1}{2} \ln \frac{1+v}{1-v}$. Notice that if we apply two boosts

to the coordinates of parameters ψ_1 and ψ_2 the results is a boost $\psi_1 + \psi_2$. Thus, we can easily apply multiple boosts of specified parameters and follow those changes in light-cone coordinates.

Rapidity is a kinematic variable that provides a more natural way to describe the motion of relativistic particles than velocity [6]. It is defined as

$$y = \frac{1}{2} \ln \left(\frac{E + p_z}{E - p_z} \right) \tag{16}$$

The rapidity variable is particularly useful in high-energy physics because, unlike velocity, it transforms additively under Lorentz boosts. If a particle with rapidity y is boosted by ψ, its new rapidity is simply:

$$y' = y + \psi \tag{17}$$

This property greatly simplifies calculations in collider experiments, where particles and reference frames experience multiple boosts. In experimental settings, pseudo-rapidity η is often used instead of rapidity because it depends only on the angle of a particle relative to the beam axis:

$$\eta = -\ln \tan \frac{\theta}{2} \tag{18}$$

For massless or highly energetic particles, η and y are nearly identical, making pseudo-rapidity a convenient experimental proxy for rapidity.

One of the reasons rapidity is so useful in high-energy physics is that the distribution of final-state particles in hadronic collisions is often approximately uniform in rapidity. This means that analyzing data in terms of rapidity rather than standard spatial coordinates provides a clearer picture of the underlying dynamics.

For example, in a proton-proton collision, the produced hadrons tend to be uniformly distributed in rapidity, which suggests that rapidity and transverse momentum are the most natural variables for analyzing jet structures.

In the context of the application, a boost is conditioned to bring the new reference frame to $V^+ = AV^-$, where A is a constant. The simple and defined forms of boosts and rapidity in light-cone coordinates make automated calculations to a new reference frame with the laid-out conditions possible. A formula for the rapidity and transformation can be derived as a function of the original vector components.

CHAPTER 2

MATLAB APPLICATION PROCESS AND FUNCTION

2.1 APPLICATION COMPONENTS AND FUNCTION

The purpose of the application I built with MATLAB application designer is to use two four-vectors specified by the user in the lab frame to define a new reference frame and determine the transformation matrix. Then, the user may supply up to four additional different vectors to be transformed into the new reference frame, where they may be plotted and visualized exactly, and the effects of the transformation on various approximations may be understood. The vectors in both the original and transformed frames will be plotted and compared.

Two reference vectors must be specified in the lab frame to establish a unique new reference frame. Just one vector can be aligned along a specified axis (z-axis), and this partially defines a new reference frame, but there remains the freedom to rotate this system around the z-axis. Thus, a second vector aligned on a plane will specify the rotation and complete the specification of the new reference frame. In my notation, the first vector, V, will be aligned to the z-axis. The second vector, Y, will be aligned to the xz-plane.

$$V^{\mu} = (V^0, V^x, V^y, V^z) \rightarrow V'^{\mu} = (V'^0, 0, 0, V'^z) \tag{19}$$

$$Y^{\mu} = (Y^0, Y^x, Y^y, Y^z) \rightarrow Y'^{\mu} = (Y'^0, Y'^x, 0, V'^z) \tag{20}$$

The procedure of the application is to apply the transformation outlined above to various vectors as defined by the user, either by direct input of the individual vector components or parametrically. The application's layout is divided into input and output/plot.

The new reference frame is defined to be boosted such that $V^{+} = AV^{-}$. As an example, the value of the constant A will equal ten in our sample calculations, but any nonzero value is allowed. A boost and multiple rotation matrices are applied to the original vectors to transform the two vectors in the new reference frame completely.

Solving for components for the final transformation matrix in terms of the original vector components, we found the transformation matrix,

$$L^{\mu}{}_{v} = \begin{bmatrix} \frac{1}{2}e^{y_T-y_r}(1+\frac{V_z}{v}) & \frac{1}{2}e^{y_T-y_r}(1-\frac{V_z}{v}) & \frac{e^{y_T-y_r}V_x}{v\sqrt{2}} & \frac{e^{y_T-y_r}V_y}{v\sqrt{2}} \\ \frac{1}{2}e^{y_T-y_r}(1-\frac{V_z}{v}) & \frac{1}{2}e^{y_T-y_r}(1+\frac{V_z}{v}) & -\frac{e^{y_T-y_r}V_x}{v\sqrt{2}} & -\frac{e^{y_T-y_r}V_y}{v\sqrt{2}} \\ -\frac{V_x}{\widetilde{v}\sqrt{2}} & \frac{V_x}{\widetilde{v}\sqrt{2}} & \frac{V_z}{\widetilde{v}} & 0 \\ -\frac{V_yV_z}{v\widetilde{v}\sqrt{2}} & \frac{V_yV_z}{v\widetilde{v}\sqrt{2}} & -\frac{V_yV_x}{v\widetilde{v}} & \frac{v}{\widetilde{v}} \end{bmatrix}. \tag{21}$$

The abbreviation used in the matrix are defined as

$$v = \sqrt{V_x^2+V_y^2+V_z^2}\,, \tag{22}$$

$$\widetilde{v} = \sqrt{V_x^2+V_z^2}\,, \tag{23}$$

$$e^{2y_T} = A\,, \tag{24}$$

$$e^{2y_r} = \left|\frac{V_0+v}{V_0-v}\right|. \tag{25}$$

One result of this project is a compact expression for this transformation that can be used with any choice of variables. The above matrix will transform the V and Y vectors into the new reference frame. V will be aligned along the z-axis, and to fully specify the frame, one final rotation will align Y on the xz-plane:

$$R^{\mu}{}_{\nu} = \begin{pmatrix} 1 & 0 & 0 & 0 \\ 0 & 1 & 0 & 0 \\ 0 & 0 & f & \sqrt{1-f^2} \\ 0 & 0 & -\sqrt{1-f^2} & f \end{pmatrix}. \tag{26}$$

Some other useful abbreviations are

$$Y_L{}^x = \frac{V^z Y^x - V^x Y^z}{\tilde{v}} \tag{27}$$

$$Y_L{}^y = \frac{V^{x2} Y^y - V^x V^y Y^x + V^z (V^z Y^y - V^y Y^z)}{\tilde{v} v} \tag{28}$$

$$f = \frac{Y_L^x / Y_L^y}{\sqrt{1 + \frac{Y_L^{x\,2}}{Y_L^{y\,2}}}} \tag{29}$$

$$\tilde{f} = \sqrt{1 - f^2} \tag{30}$$

$$\Delta = y_T - y_r \tag{31}$$

$$R^+ = 1 + \frac{V^z}{v} \tag{32}$$

$$R^- = 1 - \frac{V^z}{v}\,. \tag{33}$$

Combining the two transformation matrices, we get the complete matrix to transform to the new reference frame:

$$\Lambda^\mu{}_\nu = R^\mu{}_{\nu'} L^{\nu'}{}_\nu \tag{34}$$

with

$$\Lambda^\mu{}_\nu = \begin{pmatrix} \frac{1}{2} e^{\Delta} R^+ & \frac{1}{2} e^{\Delta} R^- & e^{\Delta} \frac{V^x}{v\sqrt{2}} & e^{\Delta} \frac{V^y}{v\sqrt{2}} \\ \frac{1}{2} e^{-\Delta} R^- & \frac{1}{2} e^{-\Delta} R^+ & -e^{-\Delta} \frac{V^x}{v\sqrt{2}} & -e^{-\Delta} \frac{V^y}{v\sqrt{2}} \\ -\frac{V^x}{\tilde{v}\sqrt{2}} f - \tilde{f} \frac{V^y V^z}{v\tilde{v}\sqrt{2}} & \frac{V^x}{\tilde{v}\sqrt{2}} f + \tilde{f} \frac{V^y V^z}{v\tilde{v}\sqrt{2}} & \frac{V^z}{\tilde{v}} f - \tilde{f} \frac{V^y V^z}{v\tilde{v}} & \tilde{f} \frac{\tilde{v}}{v} \\ \frac{V^x}{\tilde{v}\sqrt{2}} \tilde{f} - f \frac{V^y V^z}{v\tilde{v}\sqrt{2}} & -\frac{V^x}{\tilde{v}\sqrt{2}} \tilde{f} + f \frac{V^y V^z}{v\tilde{v}\sqrt{2}} & -\frac{V^z}{\tilde{v}} \tilde{f} - f \frac{V^y V^z}{v\tilde{v}} & f \frac{\tilde{v}}{v} \end{pmatrix} \tag{35}$$

These equations form the basis for the base code that operates in the MATLAB

application.

2.1.1 INPUT

The left-hand side of the application window hosts dialog boxes for the individual four-vector Cartesian coordinates for the various vectors. There are 6 vectors to input component values for: the V and Y vectors that are the basis for the new reference frame, and up to four candidate W vectors to transform to the new frame shown in Figure 4. In practice, these extra W vectors will usually correspond to other momentum, coordinate, and/or spin vectors that are involved in the process. For instance, it could be input to represent the momentum of one of the extra quarks not directly involved in the production of the hadron or jet. The interface informs the user of vector categories with bold headings. Each vector's text is also color-coded to the same color that the vector will appear on the output plots. To insert a vector component value, the user must select the desired dialog box with their mouse cursor and input a numeric value. The application will automatically process the change. The user does not need to press a button or keybind to update the output of the application.

The first W vector is always enabled, making sure the user has at least one candidate vector to examine. Some buttons enable the subsequent W vectors, and all of the previous W vectors need to be enabled to enable the next one. Checking the 'Add 2nd W Vector' button will allow the W_2^μ to be edited, and the same for the third and fourth candidate vectors. When a vector is enabled, it will be transformed to the new reference frame. It will also appear on both output plots on the right-hand side of the application's interface.

Instead of directly inputting the value for a vector component, the user can click the 'P' button beside one of the reference vector's components to open another application window to generate a value parametrically. Details about this process are discussed in Section 2.2.1.

Output

The right-hand side of the application window houses the two 3-D plots to output the vectors. In Figure 4, the top plot titled "Original Vectors" plots the original V^μ, Y^μ, and selected W_i^μ. The bottom plot will output the vectors in the new reference frame. In Figure 4, the red vector, V^μ, is transformed to align along the z-axis, and

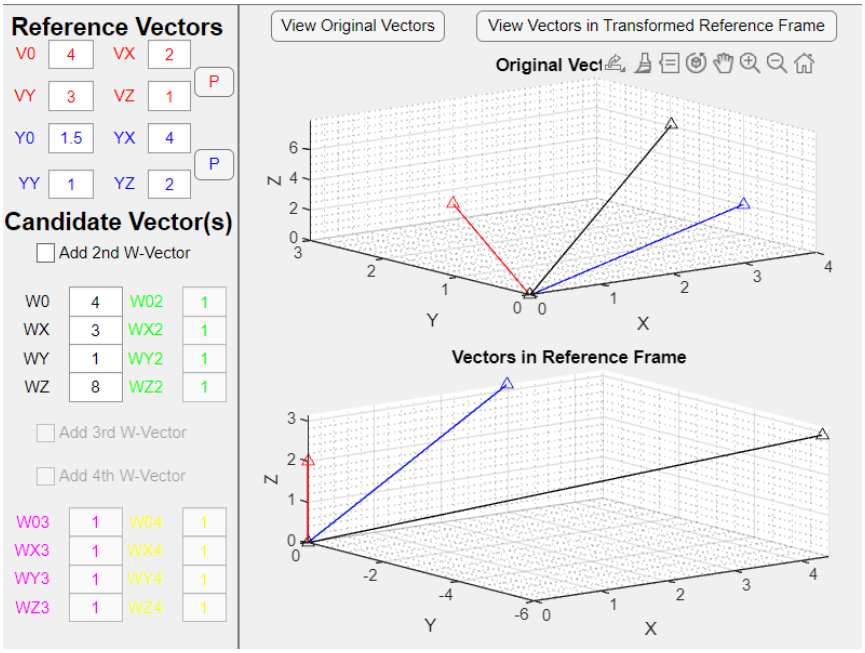

FIG. 4: The Main Application Window with input on the left and output plots on the right. V and Y are located at the top left of the window, under the 'Reference Vectors' header. To edit the components for the W_2, W_3, and W_4 vectors, the corresponding 'Add n-th W-vector' checkbox must be checked. On the output side, the top plot displays the vectors in the original lab frame, and the bottom plot represents the vectors in the new transformed frame. Only the vectors enabled in the input section will be displayed on the two plots.

the blue vector, Y^μ, lies on the xz-plane to complete the reference frame. In addition to the plots, four dialog boxes output the zero component of the transformed vectors for V^μ, Y^μ, W_1^μ, and W_2^μ. This is because the zero component of the four-vector is not visible in the 3D vector plot.

The user can hover over the top right corner of both plots to select various viewing tools. These include a pan, rotation, zoom in, and zoom out of the 3D space. To get the exact component values of each vector in the transformed frame, the user can hover over the head of the desired vector, and a small box will appear with the x, y, and z components of the vector. If the user clicks the head of the vector, the box will lock in view on the plot.

2.2 OTHER APPLICATIONS CALLED BY THE MAIN APPLICATION

2.2.1 PARAMETRIZATION

To the right of the reference vectors in the input section of the main application, there are two buttons labeled 'P' for parameters. When the user clicks on one of the buttons, an additional application window will open. That window will allow the user to enter values for parameters that will be used to obtain values for the components of the reference vectors. For example, in Figure 5, the application has input boxes for the magnitude, direction, and energy of two hadron momentum vectors. The corresponding unit vectors will be generated accordingly. When the user clicks the 'apply' button, the window will close, and the reference vector will update based on a defined formula based on the parameters in the code.

2.2.2 2D VECTOR PROJECTIONS

At the top of the output section of the main application window, there are buttons to view the 2D projections of the displayed vectors before and after the transformation. This feature can help visualize angles between vectors or their values in certain 2D planes.

2.3 DEMONSTRATIONS

The process we use for illustration is electron-positron colliding and annihilating

at high center-of-mass energy, producing two hadrons in the final state and unobserved "X" states

$$e^+(l)e^-(l') \longrightarrow h_1(p_1)h_2(p_2) + X\,. \tag{36}$$

In the lab center-of-mass frame, the virtual photon momentum q has zero momentum and energy Q,

$$q_\gamma = l_\gamma + l'_\gamma = (Q, \mathbf{0}) = \left(\frac{Q}{\sqrt{2}}, \frac{Q}{\sqrt{2}}, \mathbf{0}_{\rm T}\right)_{\text{light cone variables}}\,. \tag{37}$$

The γ subscripts mean the components are in the lab (or "photon") frame. The two hadrons' momenta, based on their energies and 3-vector magnitudes, are

$$p_{1,\gamma} = (E_{1,\gamma}, |\mathbf{p}_{1,\gamma}|\mathbf{n}_{1,\gamma})\,, \qquad p_{2,\gamma} = (E_{2,\gamma}, |\mathbf{p}_{2,\gamma}|\mathbf{n}_{2,\gamma})\,. \tag{38}$$

In lightcone variables, the momenta are

$$p_{1,\gamma} = \frac{1}{\sqrt{2}}|\mathbf{p}_{1,\gamma}|\left(\frac{E_{1,\gamma}}{|\mathbf{p}_{1,\gamma}|} + n_{z1,\gamma}, \frac{E_{1,\gamma}}{|\mathbf{p}_{1,\gamma}|} - n_{z1,\gamma}, \mathbf{n}_{T1,\gamma}\sqrt{2}\right), \tag{39}$$

$$p_{2,\gamma} = \frac{1}{\sqrt{2}}|\mathbf{p}_{2,\gamma}|\left(\frac{E_{2,\gamma}}{|\mathbf{p}_{2,\gamma}|} + n_{z2,\gamma}, \frac{E_{2,\gamma}}{|\mathbf{p}_{2,\gamma}|} - n_{z2,\gamma}, \mathbf{n}_{T2,\gamma}\sqrt{2}\right)\,. \tag{40}$$

The n vectors are unit 3-vectors,

$$||\mathbf{n}_{1,\gamma}|| = ||\mathbf{n}_{2,\gamma}|| = 1\,. \tag{41}$$

An alternative photon frame, called the Collins-Soper frame, is rotated from the lab frame to align the hadrons conveniently. We define X and Z four-vectors,

$$X^\mu = \frac{(0, \mathbf{n}_{1,\gamma} + \mathbf{n}_{2,\gamma})}{|\mathbf{n}_{1,\gamma} + \mathbf{n}_{2,\gamma}|}, \qquad Z^\mu = \frac{(0, \mathbf{n}_{1,\gamma} - \mathbf{n}_{2,\gamma})}{|\mathbf{n}_{1,\gamma} - \mathbf{n}_{2,\gamma}|}\,. \tag{42}$$

The x and z axes are taken to be the spatial components of X^μ and Z^μ, and the y axis follows from the right-hand rule. The Collins-Soper frame is useful for applications where a pair of measured hadrons (say, pions) have nearly momenta that are nearly equal in magnitude but opposite in directions. See, for example, Section 13.2 of Ref. [7]. Then, the transverse component of q becomes a measure of slight deviations from back-to-back.

In units where energy is GeV/c^2 and the speed of light is $c = 1$, the lab frame four-vectors for this transformation to be used for illustration are defined as

$$p_{1,\gamma} = (0.5, 0.5\mathbf{n}_{1,\gamma}) \text{ GeV} \tag{43}$$

$$p_{2,\gamma} = (0.99, \mathbf{n}_{2,\gamma}) \text{ GeV} \tag{44}$$

$$\mathbf{n}_{1,\gamma} = (0.4738, 0.508, 0.7193) \tag{45}$$

$$\mathbf{n}_{2,\gamma} = -(0.75, 0.433, 0.5)\,. \tag{46}$$

I have taken the $\mathbf{n}$ vectors to be nearly equal in magnitude but opposite in sign, similar to what is illustrated schematically in Figure 3, to evoke a typical case dealt with by the Collins-Soper frame.

Figure 5 shows the input parameters for the hadron momenta to transform from the lab frame to the Collins-Soper frame [7]. All momentum and energy components are in units of GeVs. The two direction angles define the components of the unit vectors. The unit vectors are then substituted in Equation 42 to generate the X^μ and Z^μ vectors.

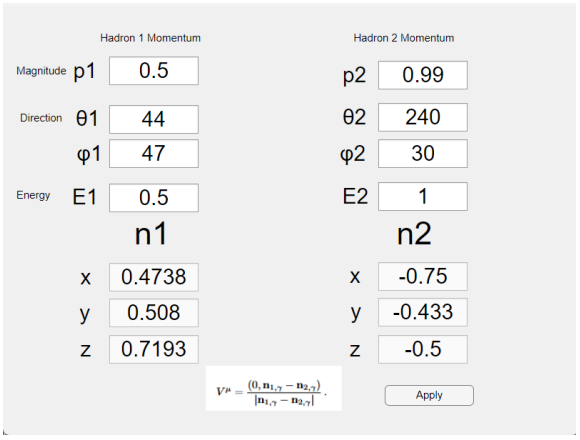

FIG. 5: Parameters of two hadrons in transformation from the lab frame to the Collins-Soper frame. The two direction angles for the momenta determine the n_1 and n_2 vectors. Both momenta and energies are in units of GeV and $c = 1$.

The next step is to see how the transformation affects vectors other than the ones we used to define the transformation. These could be, for example, momenta for other quarks, gluons, or hadrons in the collision process. I will call any such other vectors in the transformation process "candidate" vectors. The first candidate W^μ vector can be considered a quark moving along the direction of $\boldsymbol{p_1}$ with a smaller

magnitude, which could represent one of the dotted vectors in Figure 3, defined as

$$W_1^\mu = (0.1, 0.1\,\mathbf{w}_{1,\gamma})\,\mathrm{GeV} \tag{47}$$

$$\mathbf{w}_{1,\gamma} = \left(0.5, 0.5, \frac{\sqrt{2}}{2}\right). \tag{48}$$

Throughout the rest of this text, I will use units where $c = 1$. The second candidate W^μ vector is the second defined hadron momentum used to obtain the X^μ and Z^μ vectors,

$$W_2^\mu = p_{2,\gamma}^\mu\,. \tag{49}$$

In the lab frame, it is transformed to the Collins-Soper frame. Using the definitions of X^μ and Z^μ in Eq. (42), I generated the desired Y^μ and V^μ vectors, respectively, for the transformations using the application. In Figure 6, the transformation with the parameters from Figure 5 is displayed in the main application window. The two W^μ vectors defined in Eqs. (47,49) are shown in the original vector output plot by the black and green vectors, respectively. Then, the application transforms the vectors to the Collins-Soper frame defined by X^μ and Z^μ in Eq. (42). Figure 7 shows the 2-D projections of each vector present in the Figure 6 plots.

An additional frame worth considering as an example is the so-called "hadron-frame." One complication it will highlight is that the transformation matrix in Eq.(35) is insufficient to account for all possible reference frames one might hope to consider. However, it will also illustrate how any reference frame can be formed from a combination of Eq.(35) transformations. The hadron frame is a frame where the hadrons move exactly along the z-axis with no transverse (x or y) components [8]. We will indicate it with H subscripts. The virtual photon has zero rapidity, meaning that in this frame, the virtual photon has no momentum in the z-direction. Thus,

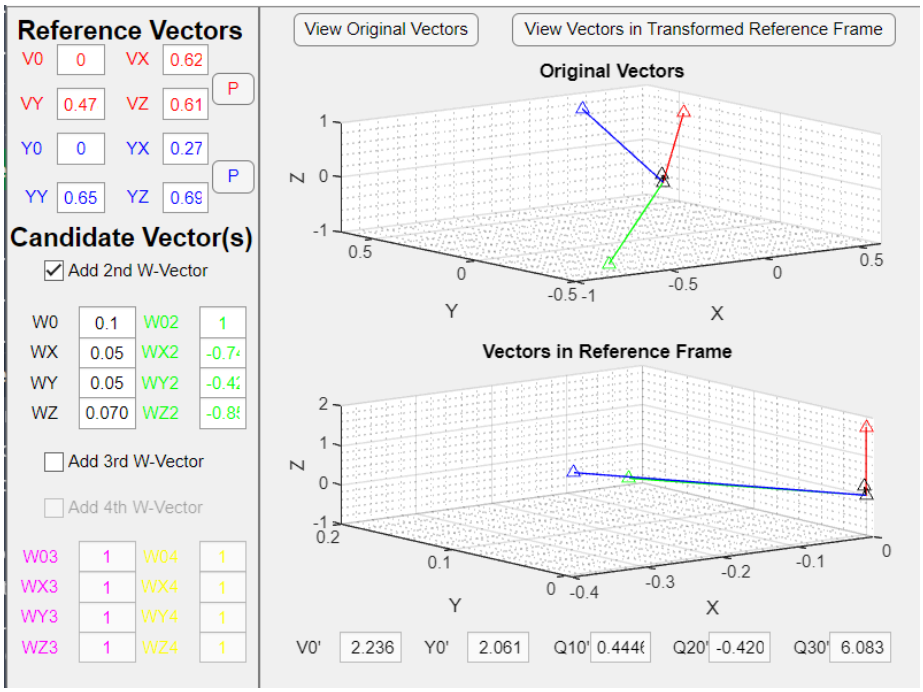

FIG. 6: Application Window of Transformation from the Lab frame to the Collins-Soper frame. Lab frame plot: the rightmost (red) is Z^μ, the leftmost (blue) is X^μ, p_2 (green) is pointing in the negative direction, and the small middle vector is the quark (black). Collins-Soper frame: Z^μ is aligned to z-axis, p_2 is second-largest vector, X^μ is largest vector, quark is the smallest vector

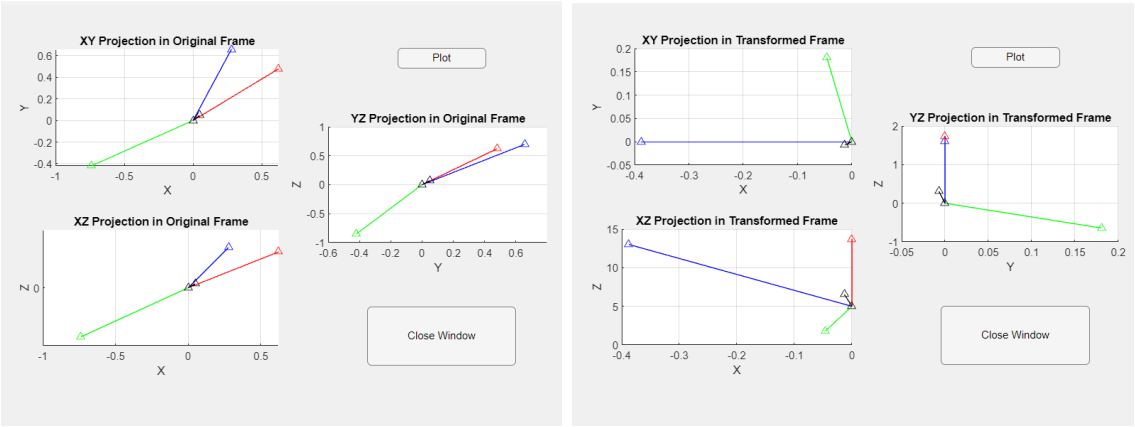

FIG. 7: (left) 2D projections of vectors in lab frame: Z^μ is the rightmost (red) vector on the XY and XZ projections, the quark is the smallest vector (black) on each plot, X^μ is the rightmost (blue) vector on the YZ projection, p_2 (green) is the vector with negative components. (right) 2D projections of vectors in Collins-Soper frame: Z^μ aligned to z-axis, X^μ is on xz-plane, quark is the smaller vector, p_2 is the other remaining vector.

$q_H^+ = q_H^-$. The momenta in the hadron frame in light-cone variables are

$$q_H = \left(q_H^+, q_H^+, \boldsymbol{q}_{H,\mathrm{T}}\right) = \left(\sqrt{\frac{Q^2+q_{H,\mathrm{T}}^2}{2}}, \sqrt{\frac{Q^2+q_{H,\mathrm{T}}^2}{2}}, \boldsymbol{q}_{H,\mathrm{T}}\right) , \tag{50}$$

$$p_{1,H} = \left(p_{1,H}^+, \frac{m_1^2}{2p_{1,H}^+}, \mathbf{0}_{H,\mathrm{T}}\right) = \left(\xi_1 q_H^+, \frac{m_1^2}{2\xi_1 q_H^+}, \mathbf{0}_{\mathrm{T}}\right) , \tag{51}$$

$$p_{2,H} = \left(\frac{m_2^2}{2p_{2,H}^-}, p_2^-, \mathbf{0}_{H,\mathrm{T}}\right) = \left(\frac{m_2^2}{2\xi_2 q_H^-}, \xi_2 q_H^-, \mathbf{0}_{H,\mathrm{T}}\right) . \tag{52}$$

We have defined for convenience the boost-invariant momentum fractions,

$$\xi_1 \equiv \frac{p_{1,H}^+}{q_H^+} = \frac{p_1\cdot q}{Q^2+q_{H,\mathrm{T}}^2} + \sqrt{\left(\frac{p_1\cdot q}{Q^2+q_{H,\mathrm{T}}^2}\right)^2 - \frac{m_1^2}{Q^2+q_{H,\mathrm{T}}^2}} , \tag{53}$$

$$\xi_2 \equiv \frac{p_{2,H}^-}{q_H^-} = \frac{p_2\cdot q}{Q^2+q_{H,\mathrm{T}}^2} + \sqrt{\left(\frac{p_2\cdot q}{Q^2+q_{H,\mathrm{T}}^2}\right)^2 - \frac{m_2^2}{Q^2+q_{H,\mathrm{T}}^2}} . \tag{54}$$

The expressions after the second equals sign provide Lorentz invariant definitions for the lightcone momentum fractions. In general, the square roots could have minus signs in front of them. We keep the plus signs because this gives a back-to-back configuration when $m_1^2/Q^2, m_2^2/Q^2 \to 0$ with the z-axis lying along the direction of hadron 1. Notice also that

$$2p_1\cdot p_2 = 2\xi_1\xi_2 q_H^+ q_H^- + \frac{m_1^2 m_2^2}{2\xi_1\xi_2 q_H^+ q_H^-} = \left(Q^2+q_{H,\mathrm{T}}^2\right)\xi_1\xi_2 + \frac{m_1^2 m_2^2}{\xi_1\xi_2\left(Q^2+q_{H,\mathrm{T}}^2\right)} . \tag{55}$$

If we take masses to be small relative to Q, then

$$2p_1\cdot p_2 = \xi_1\xi_2\left(Q^2+q_{H,\mathrm{T}}^2\right) , \tag{56}$$

$$2p_1\cdot q = \xi_1\left(Q^2+q_{H,\mathrm{T}}^2\right) , \tag{57}$$

$$2p_2\cdot q = \xi_2\left(Q^2+q_{H,\mathrm{T}}^2\right) . \tag{58}$$

So,

$$\xi_1 \approx \frac{p_1\cdot p_2}{p_2\cdot q}, \qquad \xi_2 \approx \frac{p_1\cdot p_2}{p_1\cdot q} . \tag{59}$$

Let us define two more vectors,

$$P \equiv p_1 - p_2 \qquad R = p_1 + p_2 \,. \tag{60}$$

In the hadron frame,

$$P_H = \left(\xi_1 q_H^+ - \frac{m_2^2}{2\xi_2 q_H^-}, \frac{m_1^2}{2\xi_1 q_H^+} - \xi_2 q_H^-, \mathbf{0}_{H\mathrm{T}} \right) , \tag{61}$$

$$R_H = \left(\xi_1 q_H^+ + \frac{m_2^2}{2\xi_2 q_H^-}, \frac{m_1^2}{2\xi_1 q_H^+} + \xi_2 q_H^-, \mathbf{0}_{H\mathrm{T}} \right) \tag{62}$$

Now we can start in the lab frame and use the application to look at vectors in the Collins-Soper and hadron frames. In the first case, Z will correspond to the V vector and X will correspond to the Y vector. In the hadron frame case, we will use two steps.

1. First, use R as the V vector and p_2 as the Y vector. We will use $A = 1$ to align the R to the z-axis and ensure the p_2 and p_1 will have the same x-components in magnitude and equal angles to the x-axis. This will ensure the sum and difference of the two vectors align on the z-axis in the transformation to the hadron frame.

   The result will be a vector corresponding to Eq. (61), but p_1 and p_2 may have nonzero transverse components.

2. Repeat step 1, but using the output vectors of step 1 as input. Let the vectors with components resulting from step 1 be labeled with an H' subscript. Then, in the second step, use $P_{H'}$ as the input V vector and $q_{H'}$ as the input Y vector. For the second step, use

$$A = \frac{P_H^+}{P_H^-} = \frac{2\xi_1^2 \xi_2 {q_H^+}^2 - \xi_1 \xi_2 m_2^2}{2\xi_1 \xi_2^2 {q_H^+}^2 - \xi_1 \xi_2 m_1^2} = \frac{2\xi_1 \left(Q^2 + q_{H,\mathrm{T}}^2 \right) - m_2^2}{2\xi_2 \left(Q^2 + q_{H,\mathrm{T}}^2 \right) - m_1^2} \,. \tag{63}$$

   This will give the final hadron frame components.

For an example for the transformation from the lab frame to the hadron frame using

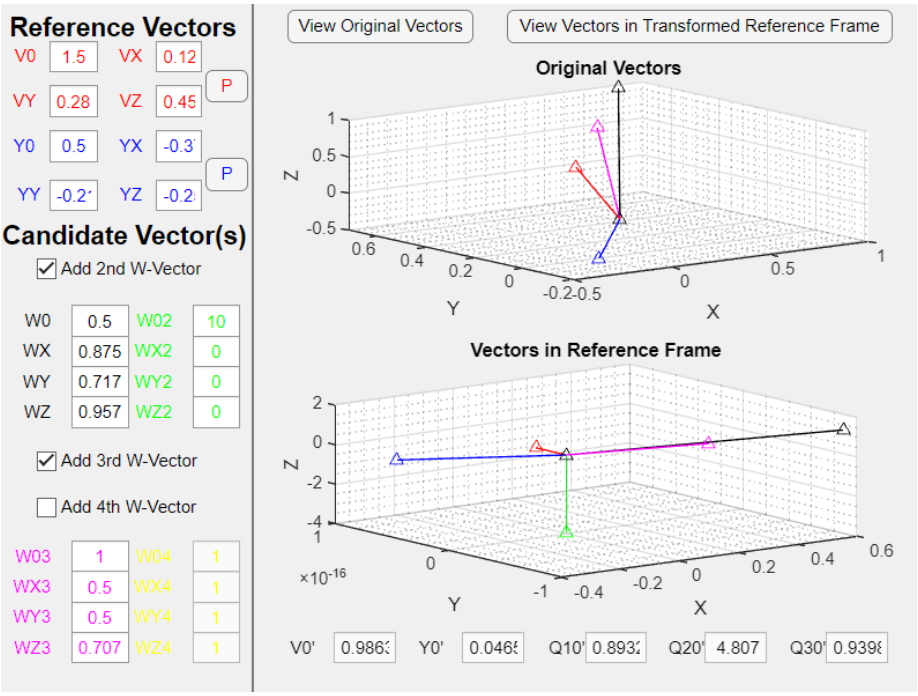

FIG. 8: Transformation from lab frame in Eqs. (63-70) to H' frame. Lab frame from bottom to top in clockwise order: p_2 (blue), R (red), p_1 (magenta), P (black), q (green) is not visible. H' frame: R is aligned to z-axis, p_2 is the left vector, P is the larger right vector, q is vertical vector, p_1 is the smaller right vector.

my application. I defined the vectors in the lab frame as the following:

$$p_{1,\gamma} = (1.0, 1.0\mathbf{n}_{1,\gamma})\ \text{GeV} \tag{64}$$

$$p_{2,\gamma} = (0.5, 0.5\mathbf{n}_{2,\gamma})\ \text{GeV} \tag{65}$$

$$\mathbf{n}_{1,\gamma} = (0.5, 0.5, 0.707) \tag{66}$$

$$\mathbf{n}_{2,\gamma} = -(0.75, 0.433, 0.5) \tag{67}$$

$$q_\gamma = (Q, \mathbf{0}) \tag{68}$$

$$Q = 10\,\text{GeV} \tag{69}$$

$$m_1 = 0.1\,\text{GeV} \tag{70}$$

$$m_2 = 0.2\,\text{GeV}. \tag{71}$$

To obtain the corresponding values for ξ_1 and ξ_2, I used the approximation in Eq. (59). Then, I manipulated equation (56) to obtain the value for $\left(Q^2 + q_{H,\text{T}}^2\right)$. The

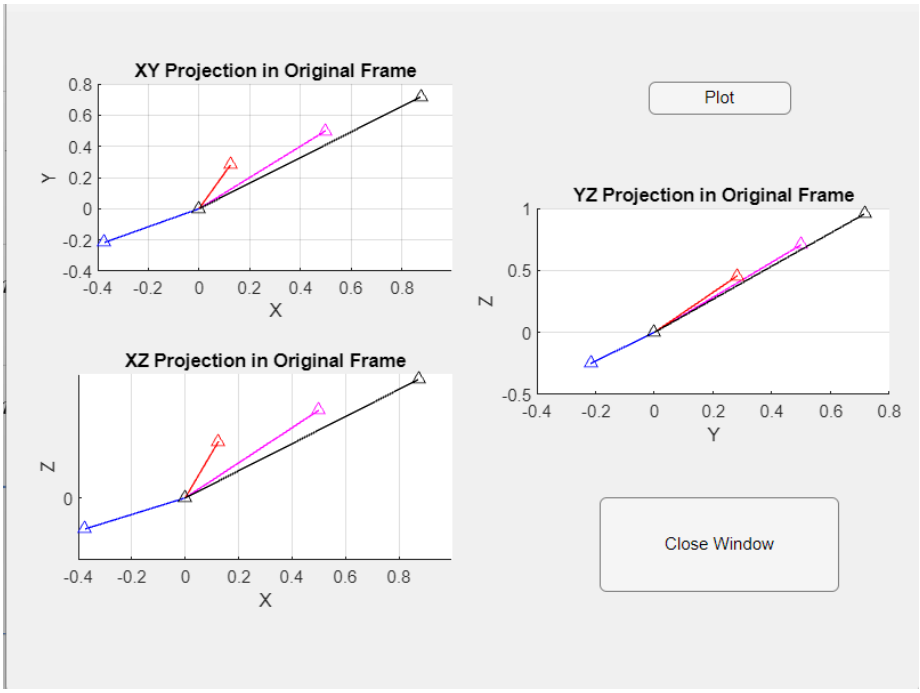

FIG. 9: 2D projections of lab frame vectors from left to right in clockwise order: p_2 (blue), R (red), p_1 (magenta), P (black), q is not pictured

values I obtained were

$$\xi_1 = 0.1945, \qquad \xi_2 = 0.0973\,,$$
$$\left(Q^2 + q^2_{H,\mathrm{T}}\right) = 10.28\ \mathrm{GeV}^2\,.$$

Finally, I determined the value needed for A in the second step of the transformation using Eq. (63), which was calculated to $A = 1.9981$. In future improvements of the application, the exact equations (53 - 55) for ξ_1, ξ_2, and $\left(Q^2 + q^2_{H,\mathrm{T}}\right)$ will be used, but the approximations are sufficient to demonstrate the hadron frame transformation simply. In Figures 8, 9 and 10, the output from step 1 is shown. The red R vector is transformed to have no 3-vector components due to how the R vector is defined in Eq. (60), the two hadron vectors become antiparallel. The exact values of the

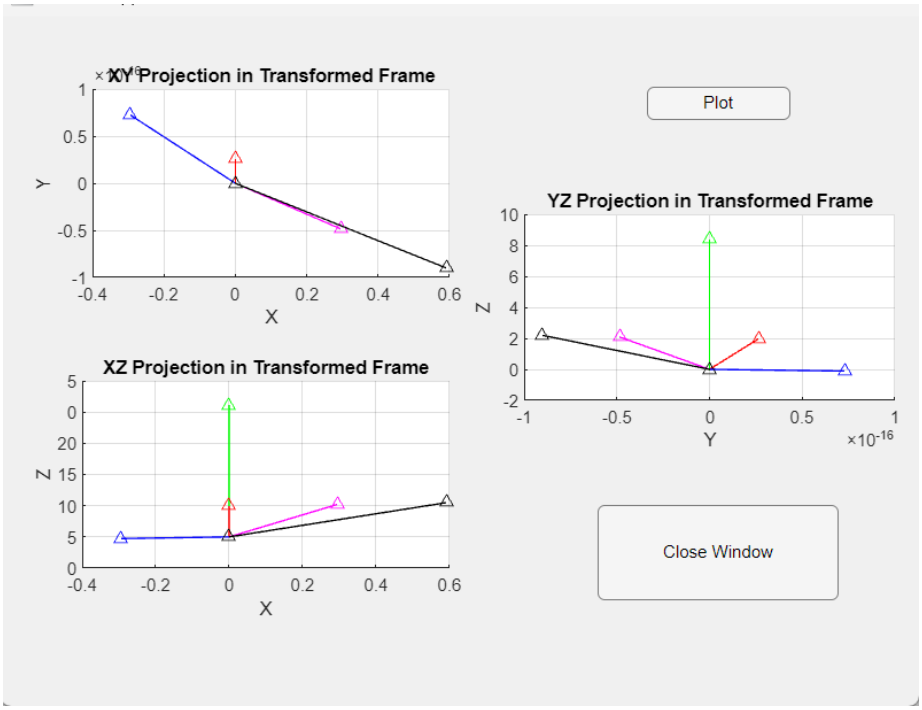

FIG. 10: 2D projections of H' frame vectors: $R_{H'}$ (red) is the smaller vector aligned to z-axis, $q_{H'}$ (green) is large vector aligned to the z-axis, $p_{2,H'}$ (blue) has the negative x-component, $P_{H'}$ (black) is the largest vector with a positive x-component, $p_{1,H'}$ (magenta) is remaining vector.

vectors in the H' frame are below:

$$p_{1,H'} = (0.9398, 0.2960, 0, 0.6315)\ \text{GeV} \tag{72}$$

$$p_{2,H'} = (0.0465, -0.2960, 0, -0.6315)\ \text{GeV} \tag{73}$$

$$P_{H'} = (0.8932, 0.5920, 0, 1.2630)\ \text{GeV} \tag{74}$$

$$R_{H'} = (0.9863, 0, 0, 0)\ \text{GeV} \tag{75}$$

$$q_{H'} = (4.807, 0, 0, -3.9567)\ \text{GeV}. \tag{76}$$

The vectors from Eqs. (72 - 76) were then applied to the application, and the rapidity in the application's code was changed to 2.0001, calculated using Eq. (63). Figure 11 shows the application window for the transformation to the hadron frame, and Figure 12 displays the hadron frame vectors. As intended, the hadron vectors and P_H and R_H are aligned along the z-axis.

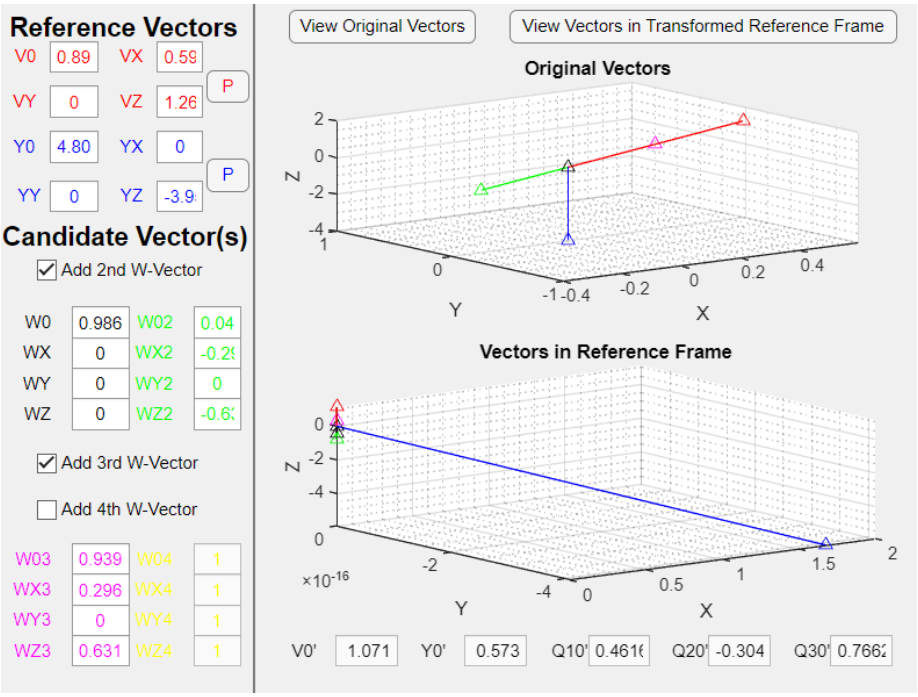

FIG. 11: Transformation from H' frame in Equations 72-76 to H frame. H' frame from most negative to most positive x-component: $p_{2,H'}$ (green), $R_{H'}$ (black), $p_{1,H'}$ (magenta), $P_{H'}$ (red); $q_{H'}$ (blue) is the vertical vector. H frame from most negative to most positive z-component: $p_{2,H}$ (green), R_H (black), $p_{1,H}$ (magenta), P_H (red); q_H (blue) is the large vector

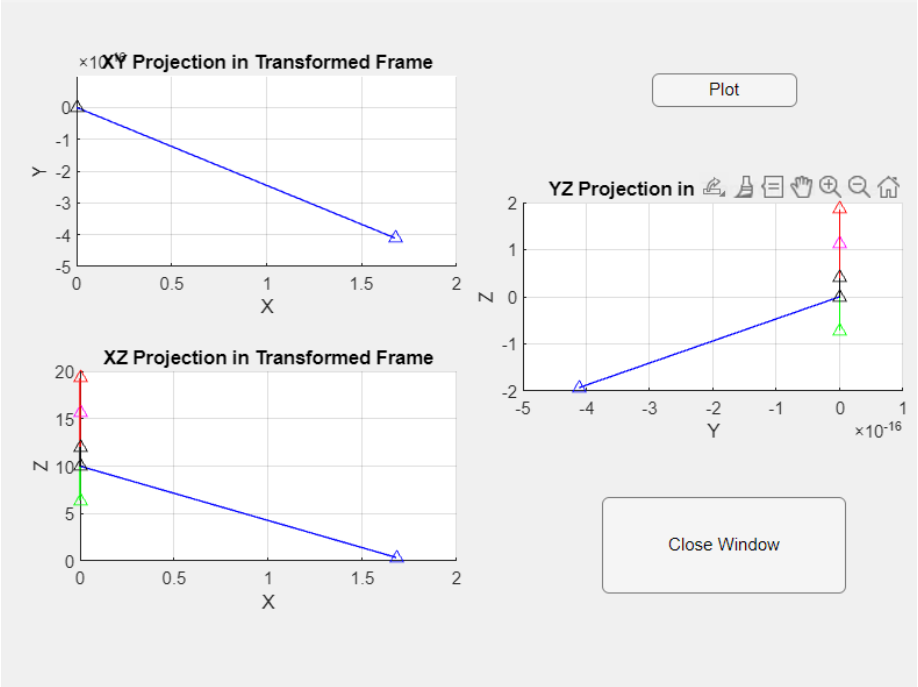

FIG. 12: 2D projections of H frame vectors from most negative to most positive z-component: $p_{2,H}$ (green), R_H (black), $p_{1,H}$ (magenta), P_H (red); q_H (blue) is the large vector with transverse components.

The vectors in the hadron frame are

$$p_{1,H} = (0.7662, 0, 0, 1.1303)\ \text{GeV}\,, \tag{77}$$

$$p_{2,H} = (-0.304, 0, 0, -0.7331)\ \text{GeV}\,, \tag{78}$$

$$P_H = (1.071, 0, 0, 1.8633)\ \text{GeV}\,, \tag{79}$$

$$R_H = (0.4616, 0, 0, 0.3971)\ \text{GeV}\,, \tag{80}$$

$$q_H = (0.573, 1.6793, 0, -5.9328)\ \text{GeV}\,. \tag{81}$$

CHAPTER 3

CONCLUSION

The primary motivation behind developing this MATLAB application was to provide a practical and efficient solution for performing reference frame transformations necessary for analyzing hadronic jets in high-energy physics. In particle and nuclear physics experiments, understanding the dynamics of jets (and other final state structures) and their originating partons requires precise transformations to frames like the Collins-Soper and hadron frames. These transformations are essential for isolating individual jet dynamics, understanding the influence of small non-perturbative effects, and applying factorization approximations accurately.

An important step in the application is the derivation of compact and adaptable transformation matrices, which can handle any choice of variables, simplifying calculations that traditionally involve complex algebraic manipulations that need to be repeated for each new physical scenario. By automating this process, the application minimizes the risk of human error and significantly speeds up the analysis, making it accessible to researchers regardless of their level of expertise in QCD formalism. This automation allows one to quickly test the approximations used in applications of factorization frameworks and approximations, making it a valuable tool for both theoretical exploration and experimental analysis of jet phenomena.

The MATLAB application I created is organized into two main sections: input and output. On the left, users input the Cartesian coordinates of vectors, including the two reference vectors, V and Y, and up to four candidate vectors, W, to be transformed. Each vector's components can be entered manually, with automatic updates displayed in the output. For more dynamic input, the application provides a parameterization feature through "P" buttons, opening a secondary window where users can input values like magnitude, direction, and energy. The right side of the application shows two 3D plots: the first visualizes the vectors in their original frame, and the second displays the transformed vectors. Users can interact with the plots to examine vector components and adjust the viewing angle. The application also offers 2D projections for better visualization of angular relationships. The combination of

user-defined input and detailed output makes the application a valuable tool for analyzing and interpreting hadronic jet phenomena in high-energy physics.

In future iterations of the application and demonstrations, exact definitions will be used, such as those for the hadron frame in Eqs. (53 - 55), in place of the approximations used for the demonstration in this document. The application can also be updated to include automatic updates of rapidity values and vectors. A potential feature could include the ability to automatically apply output from one transformation to the input vectors to perform an additional transform.

The use of the application to study specific approximations still also needs to be performed. This can start with the e^+e^--annihilation into back-to-back hadrons examples we have used for illustration. However, many other interesting cases involve complex kinematics. One is the production of "dihadrons," wherein a pair of high-speed hadrons moves in nearly the same direction as one another [9]. Another is the treatment of electromagnetic radiation in deep-inelastic scattering, where the emission of photons distorts the hadronic kinematics [10].

BIBLIOGRAPHY

[1] John C. Collins, Davison E. Soper, and George F. Sterman. Factorization of Hard Processes in QCD. Adv. Ser. Direct. High Energy Phys., 5:1–91, 1989.

[2] Frank Wilczek. QCD made simple. Phys. Today, 53N8:22–28, 2000.

[3] Andrea Banfi, Giuseppe Marchesini, and Graham Smye. Away-from-jet energy flow. Journal of High Energy Physics, 2002(08):006–006, August 2002.

[4] Andrea Banfi. Hadronic Jets: An Introduction. 2 2016.

[5] Mauro Anselmino, Harut Avakian, Alessandro Bacchetta, Aurore Courtoy, Abhay Deshpande, R. Fatemi, Leonard Gamberg, Haiyan Gao, Matthias, G. Grosse Perdekamp, Zhong-Bo Kang, S. E. Kuhn, John G. Lajoie, Hrayr, Matevosyan, Andreas Metz, Zein-Eddine Meziani, Akio Ogawa, Silvia, Pisano, Alexei Prokudin, Marco Radici, Ted C. Rogers, Patrizia Rossi, A. H. Rostomyan, Peter Schweitzer, A. Vossen, and Feng Yuan. Study of fragmentation functions in e^+e^- annihilation. 2015.

[6] J. C. Collins. Light-cone variables, rapidity and all that. 1997.

[7] J. C. Collins. Foundations of Perturbative QCD. Cambridge University Press, Cambridge, 2011.

[8] M. Boglione, A. Dotson, L. Gamberg, S. Gordon, J. O. Gonzalez-Hernandez, A. Prokudin, T. C. Rogers, and N. Sato. Mapping the Kinematical Regimes of Semi-Inclusive Deep Inelastic Scattering. JHEP, 10:122, 2019.

[9] T. C. Rogers, M. Radici, A. Courtoy, and T. Rainaldi. QCD factorization with multihadron fragmentation functions. Phys. Rev. D, 111(5):056001, 2025.

[10] Tianbo Liu, W. Melnitchouk, Jian-Wei Qiu, and N. Sato. Factorized approach to radiative corrections for inelastic lepton-hadron collisions. Phys. Rev. D, 104(9):094033, 2021.

VITA

George Vassilakopoulos
Department of Physics
Old Dominion University
Norfolk, VA 23529

George Vassilakopoulos was born in Newport News, Virginia, on February 19, 2004. He graduated from Kecoughtan High School and will earn a Bachelor of Science degree in Physics from Old Dominion University in 2025. He is also pursuing a Bachelor of Science degree in Electrical Engineering from Old Dominion University, expected to be completed in 2026. Mr. Vassilakopoulos participated in a Research Experience for Undergraduates (REU) program at Jefferson Lab in the summer of 2023, where he researched Hamiltonian Monte Carlo methods. In the summer of 2024, he participated in an REU program at Mississippi State University focusing on computational methods with applications in materials science. He has received several academic awards, including the ODU Presidential Scholarship, the Hampton Roads Community Foundation Scholarship, and the PlayVS FIFA Champion Scholarship. His research interests include high-energy and nuclear physics. Upon graduation, he plans to continue his studies in physics at the graduate level.

Typeset using LaTeX.